Electronic Supplementary Information (ESI)

Enhancing the performances of physically cross-linked photodeformable main-chain azobenzene poly(ester-amide)s via chemical structure engineering

Yan Zhou, Lei Wang and Huiqi Zhang*

State Key Laboratory of Medicinal Chemical Biology, Key Laboratory of Functional Polymer Materials (Ministry of Education), Collaborative Innovation Center of Chemical Science and Engineering (Tianjin), and College of Chemistry, Nankai University, Tianjin 300071, China.

Materials.

Tetrahydrofuran (THF, Tianjin Jiangtian Chemicals, 99%) was refluxed over sodium and then distilled. *N*,*N*-Dimethylformamide (DMF, Tianjin Jiangtian Chemicals, 99.5%) was dried with anhydrous magnesium sulfate and then distilled under vacuum. Dichloromethane [CH_2Cl_2, Tianjin Jiangtian Chemicals, analytical grade (AR)] and chloroform ($CHCl_3$, Tianjin Chemical Reagents Wholesale Co., AR) were refluxed over calcium hydride and then distilled. Triethylamine (TEA, Tianjin Jiangtian Chemicals, 99%) was dried with anhydrous sodium sulfate and then distilled. Acrylic acid (Tianjin Damao Chemical Reagent Factory, 99.5%) was purified by distillation under vacuum. 4-((4-Hydroxy)phenylazo)benzoic acid, 4-((4-(*ω*-hydroxydecyloxy))phenylazo)benzoic acid (H6AzoC), 4-((4-(*ω*-acryloyloxydecyloxy))phenylazo)benzoic acid (A6AzoC) and *N*-hydroxysuccinimide 4-((4-(*ω*-acryloyloxyalkyloxy))phenylazo)benzoate (A6AzoS) were synthesized according to our previously reported procedure (Scheme S1) (X. Li, *et al.*, *J. Mater. Chem.*, 2009, 19, 236-245). 4-Hydroxybutyl acrylamide and 6-hydroxyhexyl acrylamide were prepared following the literature method (G. Y. N. Chan, *et al.*, *Aust. J. Chem.*, 1998, 51, 31-35). 2-Hydroxyethyl acrylamide (Tianjin Heowns Biochem Technologies, LLC, 98 %),1,2-ethanedithiol (Macklin, 97%), 1,8-diazabicyclo[5.4.0]undec-7-ene (DBU, Tianjin Heowns Biochem Technologies, LLC, 98%), *N*,*N'*-dicyclohexylcarbodiimide (DCC, Tianjin Jiangtian Chemicals, AR), 4-(dimethylamino)pyridine (DMAP, Merck, AR), acryloyl chloride (Tianjin Heowns Biochem Technologies, LLC, 98%), 2-aminoethanol (Tianjin Bohua Chemical Reagent Co. Ltd., AR),

4-amino-1-butanol (Tianjin Heowns Biochem Technologies, LLC, 97%), 6-amino-1-hexanol (Shanghai Aladdin Bio-Chem Technology Co. Ltd., 97%), hexafluoroisopropanol (Shanghai Aladdin Bio-Chem Technology Co. Ltd., 99.5%), and all the other reagents were commercially available and used without further purification unless otherwise stated.

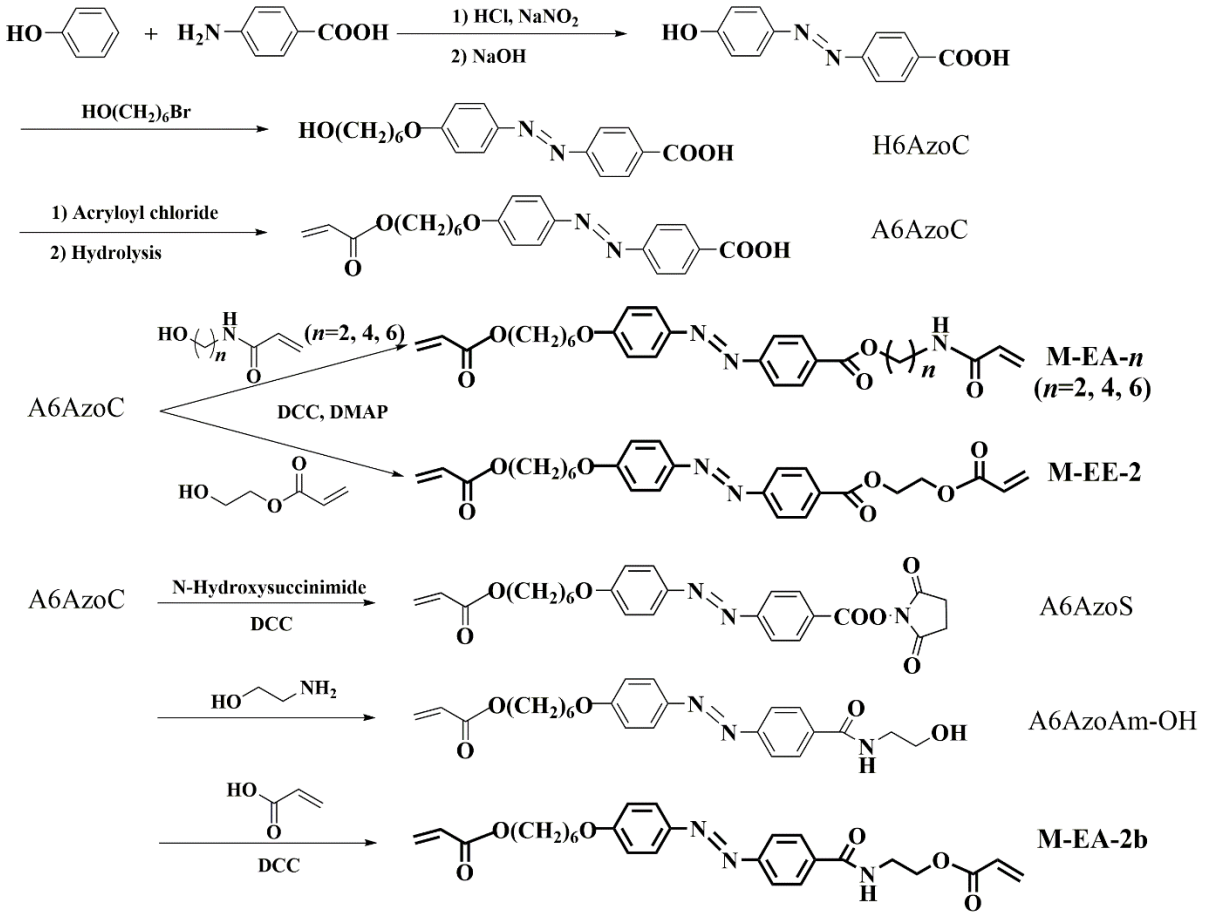

Scheme S1 Chemical structures and synthetic procedures of the azo monomers including M-EA-*n* (*n* = 2, 4, 6), M-EA-2b, and M-EE-2.

Synthesis of azo monomers with both acrylate and acrylamide end-groups and different length of flexible spacers [M-EA-*n* (*n* = 2, 6, 10), Schemes 1a and S1]

M-EA-2. A6AzoC (Scheme S1) (1.39 g, 3.50 mmol), 2-hydroxyethyl acrylamide (0.81 g, 7.00 mmol), and DMAP (85.60 mg, 0.70 mmol) were dissolved in dried CH_2Cl_2 (40 mL) and the solution was cooled down to 0 °C. To this mixture was added dropwise a solution of DCC (0.72 g, 3.50 mmol) in dried CH_2Cl_2 (10 mL) under stirring. After being magnetically stirred first at 0 °C for 1 h and then at 25 °C for 24 h, the reaction mixture was filtered and the filtrate was

evaporated to dryness under vacuum. The resulting solid was purified with silica gel column chromatography by using a mixture of petroleum ether and ethyl acetate (1:1 v/v) as the eluent, leading to an orange-yellow solid product (yield: 61 %). UV-vis [dimethylacetamide (DMAc)]: λ_{max}/nm (ε/L mol^{-1}cm^{-1}) = 362 (27489). ^{1}H NMR (400 MHz, DMSO-d_6): δ (ppm) = 8.45-8.32 (t, 1H, -CONH-), 8.22-8.10 (d, 2H, Ar-H), 8.02-7.89 (dd, 4H, Ar-H), 7.22-7.08 (d, 2H, Ar-H), 6.38-6.05 (m, 4H, CH=CH-COO- and CH=CH-CON-), 5.98-5.88 (dd, 1H, CH=C-COO-), 5.67-5.54 (dd, 1H, CH=C-CON-), 4.43-4.29 (t, 2H, Ar-COO-CH_2-), 4.18-4.00 (m, 4H, C=C-$COOCH_2$- and -CH_2-O-Ar), 3.63-3.49 (q, 2H, -CH_2-N-), and 1.85-1.33 [m, 8H, -$(CH_2)_4$-].

M-EA-4. Prepared as for M-EA-2 (yield: 56 %). UV-vis (DMAc): λ_{max}/nm (ε/L mol^{-1}cm^{-1}) = 362 (26670). ^{1}H NMR (400 MHz, DMSO-d_6): δ (ppm) = 8.20-8.07 (m, 3H, Ar-H and -NH-CO-), 7.99-7.86 (dd, 4H, Ar-H), 7.21-7.10 (d, 2H, Ar-H), 6.38-6.02 (m, 4H, CH=CH-COO- and CH=CH-CON-), 5.98-5.88 (dd, 1H, CH=C-COO-), 5.63-5.54 (dd, 1H, CH=C-CON-), 4.40-4.26 (t, 2H, Ar-COO-CH_2-), 4.18-4.04 (m, 4H, C=C-$COOCH_2$- and -CH_2-O-Ar), 3.27-3.15 (q, 2H, -CH_2-N-), and 1.85-1.33 [m, 12H, -$(CH_2)_4$- and -$(CH_2)_2$-].

M-EA-6. Prepared as for M-EA-2 (yield: 65 %). UV-vis (DMAc): λ_{max}/nm (ε/L mol^{-1}cm^{-1}) = 362 (26842). ^{1}H NMR (400 MHz, DMSO-d_6): δ (ppm) = 8.20-8.10 (d, 2H, Ar-H), 8.09-8.00 (t, 1H, -NH-CO-), 7.99-7.86 (dd, 4H, Ar-H), 7.22-7.08 (d, 2H, Ar-H), 6.38-6.00 (m, 4H, CH=CH-COO- and CH=CH-CON-), 5.98-5.88 (dd, 1H, CH=C-COO-), 5.63-5.50 (dd, 1H, CH=C-CON-), 4.40-4.25 (t, 2H, Ar-COO-CH_2-), 4.19-4.00 (m, 4H, C=C-$COOCH_2$- and -CH_2-O-Ar), 3.21-3.05 (q, 2H, -CH_2-N-), and 1.87-1.25 [m, 16H, -$(CH_2)_4$- and -$(CH_2)_4$-].

Synthesis of the diacrylate-type azo monomer with a chemical structure similar as M-EA-2 except with the exchanged position of the ester group and amide group (M-EA-2b, Schemes 1a and S1). M-EA-2b was prepared via first the synthesis of A6AzoAm-OH and its subsequent esterification reaction with acrylic acid (Scheme S1) as shown below:

Synthesis of A6AzoAm-OH (Scheme S1**).** To a solution of A6AzoS (543.1 mg, 1.1 mmol) in dried THF (5 mL) was added 2-aminoethanol (132 μL, 2.2 mmol). After being magnetically stirred at 25 ^{o}C for 5 h, the reaction mixture was evaporated to dryness under vacuum. The resulting solid was purified with silica gel column chromatography by using ethyl acetate as

the eluent, leading to an orange-yellow solid product (yield: 98%). ^{1}H NMR (400 MHz, DMSO-d_6): δ (ppm) = 8.65-8.50 (t, 1H, -CO-NH-), 8.10-8.00 (d, 2H, Ar-H), 7.97-7.83 (dd, 4H, Ar-H), 7.20-7.08 (d, 2H, Ar-H), 6.39-6.26 (dd, 1H, CH=C-), 6.23-6.09 (q, 1H, C=CH-COO-), 5.99-5.89 (dd, 1H, CH=C-), 4.80-4.68 (t, 1H, -OH), 4.20-4.04 (m, 4H, C=C-COOCH$_2$- and -CH$_2$-O-Ar), 3.60-3.48 (m, 2H, -N-C-CH$_2$-O-), 3.44-3.33 (m, 2H, -N-CH$_2$-), and 1.86-1.33 [m, 8H, -(CH$_2$)$_4$-].

Synthesis of M-EA-2b. To a cooled (at 0 ^{o}C) mixed solution of A6AzoAm-OH (439.5 mg, 1.0 mmol), acrylic acid (136 μL, 2.0 mmol), and DMAP (49.1 mg, 0.4 mmol) in dried CH_2Cl_2 (8 mL) was added dropwise a solution of DCC (413.2 mg, 2.0 mmol) in dried CH_2Cl_2 (7 mL) under stirring. The reaction mixture was magnetically stirred first at 0 ^{o}C for 1 h and then at 25 ^{o}C for 24 h. The filtrate of the above mixture was evaporated to dryness under vacuum. The resulting solid was purified with silica gel column chromatography by using a mixture of petroleum ether and ethyl acetate (1:1 v/v) as the eluent, leading to an orange-yellow solid product (yield: 90 %). UV-vis (DMAc): λ_{max}/nm (ε/L mol^{-1}cm^{-1}) = 359 (26614). ^{1}H NMR (400 MHz, DMSO-d_6): δ (ppm) = 8.89-8.70 (t, 1H, -CO-NH-), 8.10-7.96 (d, 2H, Ar-H), 7.96-7.80 (dd, 4H, Ar-H), 7.22-7.04 (d, 2H, Ar-H), 6.44-6.25 (m, 2H, CH=C-COO-), 6.25-6.06 (m, 2H, C=CH-COO-), 6.05-5.85 (m, 2H, CH=C-COO-), 4.36-4.18 (t, 2H, -N-C-CH$_2$-), 4.18-4.00 (m, 4H, C=C-COOCH$_2$- and -CH$_2$-O-Ar), 3.68-3.48 (m, 2H, -N-CH$_2$-), and 1.87-1.30 [m, 8H, -(CH$_2$)$_4$-].

Synthesis of the diacrylate-type azo monomer with a chemical structure similar as M-EA-2 except replacing the amide group with an ester group (M-EE-2, Scheme S1).

A6AzoC (396.2 mg, 1.00 mmol), 2-hydroxyethyl acrylate (232.3 mg, 2.00 mmol), and DMAP (24.5 mg, 0.20 mmol) were dissolved in dried CH_2Cl_2 (8 mL). The solution was cooled down to 0 ^{o}C, and a solution of DCC (206.5 mg, 1.0 mmol) in dried CH_2Cl_2 (6 mL) was added dropwise under stirring. After the reaction mixture was magnetically stirred first at 0 ^{o}C for 1 h and then at 25 ^{o}C for 24 h, it was filtered and the filtrate was evaporated to dryness under vacuum. The resulting solid was purified with silica gel column chromatography by using a mixture of petroleum ether and ethyl acetate (10:1 v/v) as the eluent, leading to an orange-yellow solid product (yield: 60 %). UV-vis (DMAc): λ_{max}/nm (ε/L mol^{-1}cm^{-1}) = 364 (26075).

^{1}H NMR (400 MHz, $CDCl_3$): δ (ppm) = 8.27-8.12 (d, 2H, Ar-H), 8.05-7.86 (dd, 4H, Ar-H), 7.12-6.96 (d, 2H, Ar-H), 6.54-6.35 (m, 2H, CH=C-COO-), 6.28-6.04 (m, 2H, C=CH-COO-), 5.97-5.76 (m, 2H, CH=C-COO-), 4.70-4.48 (m, 4H, Ar-COO-CH_2-CH_2-), 4.28-4.14 (t, 2H, -CH_2-O-Ar), 4.14-3.98 (t, 2H, C=C-COOCH_2-), and 1.94-1.40 [m, 8H, -$(CH_2)_4$-].

Synthesis of a main-chain azo polyester (PEE-2) (Table S1).

PEE-2 was prepared via Michael addition polymerization of M-EE-2 and 1,2-ethanedithiol in dried THF with DBU as the catalyst for 3 h as shown below: M-EE-2 (208.13 mg, 0.42 mmol), dried THF (6.75 mL), and DBU (75 μL, 0.48 mmol) were added successively into a one-neck round-bottom flask (25 mL) with a magnetic stir bar inside. After the above mixture was magnetically stirred at room temperature for 5 min, the reaction system was immersed into an ice-water bath and purged with argon for 5 min. 1,2-Ethanedithiol (36 μL, 0.42 mmol) was then added into the reaction mixture. After being purged with argon for another 20 min in an ice-water bath, the reaction system was sealed and then magnetically stirred at 60 °C for 3 h in the dark. The reaction mixture was cooled to room temperature and then precipitated into ethyl ether. The precipitate was collected by centrifugation, washed with ethyl ether thoroughly until no monomer was detectable with thin layer chromatography, and then dried at 40 °C under vacuum to the constant weight, leading to the orange-yellow main-chain azo polymer PEE-2 in a yield of 90% (Table S1, Figs. S1 and S2).

Table S1 Characterization and thermal transition data of the main-chain azo polymer PEE-2

sample [a]	yield (%)	$M_{n,NMR}$ (g mol^{-1}) [b]	$M_{n,GPC}$ (g mol^{-1}) ($Đ$) [c]	thermal transition T (°C) [d]	ΔH_{si} (J g^{-1}) [h]	T_d (°C) [i]
PEE-2	90	29400	118900 (1.86)	G 0.7 Cr 45.7 [g] Cr 74.4 Cr 85.5 I [e] I 55.1 Cr -2.4 G [f]	-5.3, 12.3, 11.0 [e] -9.3 [f]	299

[a] PEE-2 was obtained via Michael addition polymerization of M-EE-2 and 1,2-ethanedithiol with DBU as the catalyst at 60 °C for 3 h. [b] Number-average molecular weight determined by ^{1}H NMR. [c] Number-average molecular weight ($M_{n,GPC}$) and molar-mass dispersity ($Đ$) of PEE-2 were determined by GPC with THF as the eluent (polystyrene standard). [d] G = glassy, Cr = crystalline, I = isotropic. [e] DSC second heating scan under nitrogen (10 °C min^{-1}). [f] DSC first cooling scan under nitrogen (-10 °C min^{-1}). [g] Crystalline peak. [h] Enthalpy of the phase transitions. [i] The temperature at 5% weight loss of the polymer under nitrogen determined by TGA heating experiment (10 °C min^{-1}).

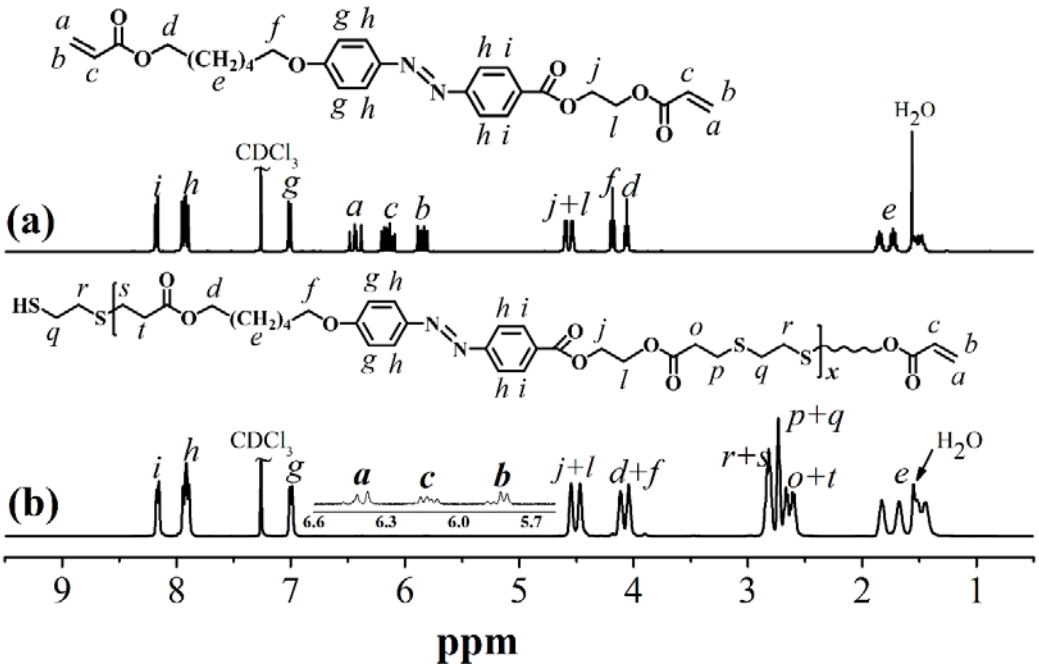

Fig. S1 ^{1}H NMR spectra of the azo monomer M-EE-2 (a) and its corresponding azo polymer (prepared via Michael addition polymerization of M-EE-2 and 1,2-ethanedithiol with DBU as the catalyst) PEE-2 (b) in $CDCl_3$ at 25 °C.

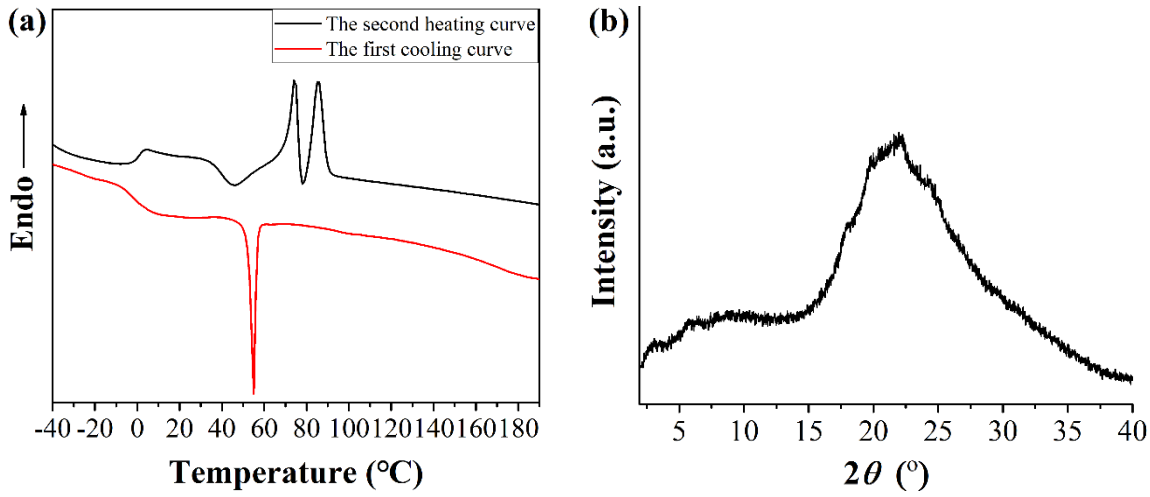

Fig. S2 (a) DSC curves of the main-chain azo polymer PEE-2 from the second heating scan and from the first cooling scan (±10 °C min^{-1}). (b) XRD spectrum of PEE-2, which was cooled from its melting state to 44 °C at a cooling rate of 10 °C min^{-1} and annealed for 1 h at 44 °C.

Characterization.

^{1}H NMR spectra of the samples were recorded on a Bruker Avance III 400 MHz NMR spectrometer.

Thermogravimetric analyses (TGA) were performed on a Netzsch TG 209 instrument under

nitrogen atmosphere at a heating rate of 10 ^{o}C min^{-1}.

Differential scanning calorimetry (DSC, Netzsch 200 F3) was used to study thermal transitions of polymers at a heating/cooling rate of 10 ^{o}C min^{-1} under nitrogen. The temperature and heat flow scale were calibrated with standard materials including indium (70-190 ^{o}C), tin (150-270 ^{o}C), zinc (350-450 ^{o}C), bismuth (190-310 ^{o}C) and mercury (-100 to 0 ^{o}C) in different temperature ranges. The glass transition temperatures (T_g) of the polymers were determined as the midpoints of the step changes of the heat capacities, while the phase transition temperatures were measured from the maximum/minimum of the endothermic/exothermic peaks.

The mesophase textures of the azo polymers and the alignment states of the polymer fibers and films were observed by using an Olympus BX51 polarizing optical microsphere (POM, with crossed polarizer and analyzer) equipped with a Linksys 32 THMSE600 hot stage and a digital camera (micropublisher 5.0 RTV).

X-ray diffraction (XRD) spectra of the azo polymers were recorded on a Rigaku SmartLab 9 kW XRD with Cu Kα radiation (1.5406 Å) at room temperature. The measured 2θ ranged from 1.5° to 40° and the scanning rate was 5 (°) min^{-1}. The azo polymer samples for XRD measurements were prepared through first heating them to a temperature above their respective melting point at a heating rate of 10 ^{o}C min^{-1}, then cooling them to 133 °C (PEA-2), 133 °C (PEA-4), 120 °C (PEA-6), 44 °C (PEE-2), 105 °C (PEA-2b) and 72 °C (PEA-2b) at a cooling rate of 10 ^{o}C min^{-1}), and finally annealing them at above temperatures for 1 h, respectively.

A Perkin Elmer Frontier FT-IR spectrometer equipped with a VT CELL GS21525 variable temperature sample cell accessory was used to carry out the variable temperature FT-IR measurements. The studied polymer samples were sandwiched between two KBr slides, and its temperature was changed at a rate of 2 °C min^{-1}.

A UV-vis scanning spectrophotometer (TU1900, Beijing Purkinje General Instrument Co., Ltd) was used to measure the UV-vis spectra of the samples and characterize the photoisomerization processes of a PEA-2 film. The PEA-2 film was cast from a PEA-2 solution in hexafluoroisopropanol (1.0 mg mL^{-1}, 200 μL) on a clean quartz glass plate (12×45 mm). After the solvent was evaporated slowly at ambient temperature for 12 h, a transparent light

yellow film was formed on the quartz glass plate. The thickness (l) of the polymer film is estimated to be 370 nm by using the equation $l = VC/\rho S$, where V is the volume of the polymer solution cast on the quartz glass plate, C is the concentration of the polymer solution, ρ is the density of the soild polymer film (ρ is assumed to be 1 g mL^{-1} here), and S is the surface area of the quartz glass plate. The photoresponsivity of the above-obtained PEA-2 thin film was studied by first irradiating it with 365 nm UV light (40 mW cm^{-2}) until its photostationary state was reached. The photostationary PEA-2 film was then irradiated with visible light (λ > 510 nm, 30 mW cm^{-2}). The UV-vis spectra of the sample were recorded during the above studies (Fig. 3). The used UV light and visible light were obtained from a Warsun Series R838 light source (a glass filter was used to obtain the desired visible light).

The order parameters of the uniaxially oriented PEA-n (n = 2, 4, 6) films (strain: 235%; thickness: ~10 μm) were determined through measuring their polarized absorption spectra by using a UV-vis scanning spectrophotometer (TU1900, Beijing Purkinje General Instrument Co., Ltd) equipped with a Glan-Taylor prism attachment. The order parameters (S) of the uniaxially oriented PEA films were derived from the equation: $S = (A_{/\!/} - A_{\perp})/(A_{/\!/} + 2A_{\perp})$, where $A_{/\!/}$ and $A_{\perp}$ represent the absorbance (at 500 nm) obtained with incident light polarized parallel and perpendicular to the stretching direction of the films, respectively (T. Ube, *et al.*, *Macromolecules*, 2022, 55, 413-420).

A NTEGRA (NT-MDT, Russia) AFM was used to characterize the surface morphologies of the PEA films in the tapping mode. The AFM tip used is a high-resolution noncontact GOLDEN silicon AFM probe (NSG01 series) with a 6 nm typical tip curvature radius.

The molecular weight and molar mass dispersity ($Đ$) of the main-chain azo polymer PEE-2 were characterized with a Waters gel permeation chromatograph (GPC) equipped with a Waters 717plus autosampler, a Waters 515 HPLC pump, a set of three Waters UltraStyragel columns (HT2, HT3, and HT4; 30 cm × 7.8 mm; 10 μm particles; exclusion limits: 100-10000, 500-30000, and 5000-600000 g/mol, respectively) (the column oven temperature was 35 °C), and a Waters 2414 refractive index detector. THF was used as the mobile phase at a flow rate of 1.0 mL/min, and the calibration curve was obtained by using polystyrene standards.

Table S2 Synthetic data of PEA-4-*t* via Michael addition polymerization of M-EA-4 and 1,2-ethanedithiol with DBU as the catalyst in THF [a]

polymerization time *t* (h)	0.15	0.25	0.5	1	3	6	12
yield (%)	65	80	90	91	90	92	90
$M_{n,NMR}$ (g mol^{-1}) [b]	2460	3690	6160	16000	28900	38200	- [c]

[a] M-EA-4 (mmol):1,2-ethanedithiol (mmol):DBU (mmol):THF (mL) = 0.14:0.14:0.16:2.25, polymerization temperature: 60 °C. [b] Absolute molecular weights of the main-chain azo PEAs determined by ^{1}H NMR. [c] The $M_{n,NMR}$ value of PEA-4-12h could not be derived from its ^{1}H NMR spectrum because of the disappearance of its acrylamide end-group signals there.

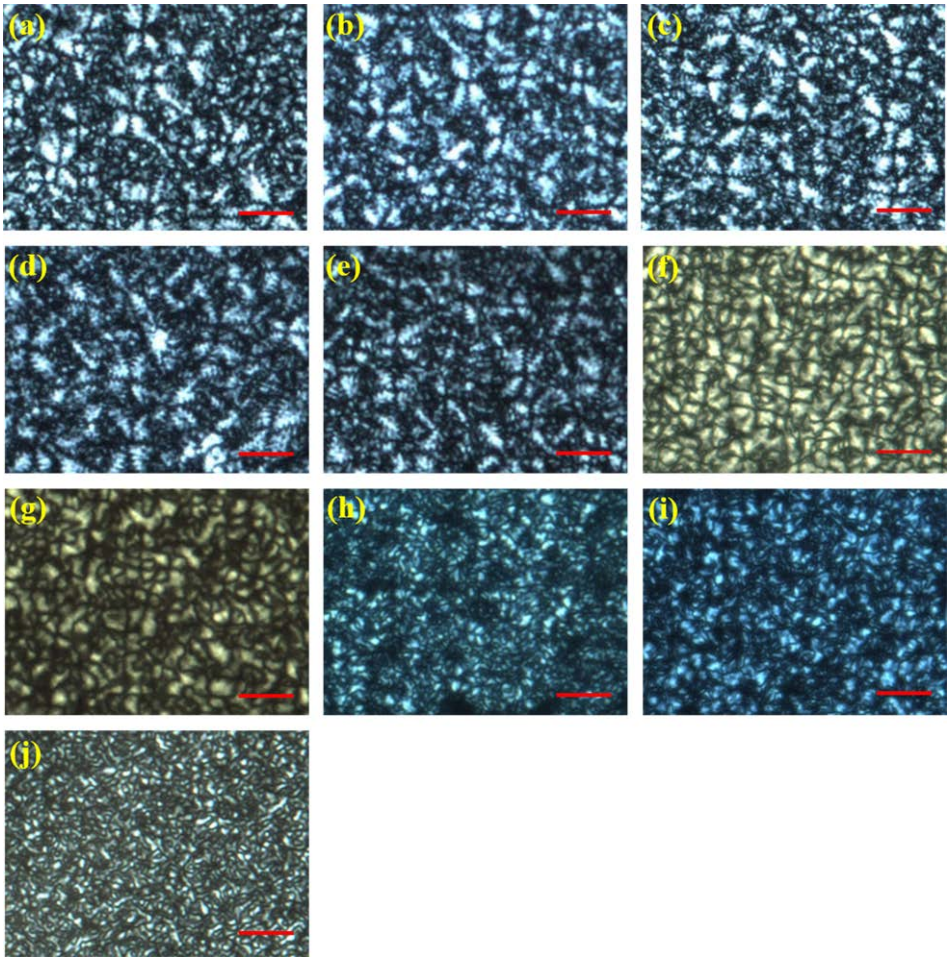

Fig. S3 POM images of the main-chain azo polymers upon cooling from the melting states to the following temperatures and then annealed for 1 h: PEA-4-0.5h at 125 °C (a), PEA-4-1h at 127 °C (b), PEA-4-3h at 133 °C (c), PEA-4-6h at 128 °C (d), PEA-4-12h at 120 °C (e), PEA-2 at 133 °C (f), PEA-6 at 120 °C (g), PEA-2b at 105 °C (h), PEA-2b at 72 °C (i), and PEE-2 at 44 °C (j). The scale bar is 20 μm.

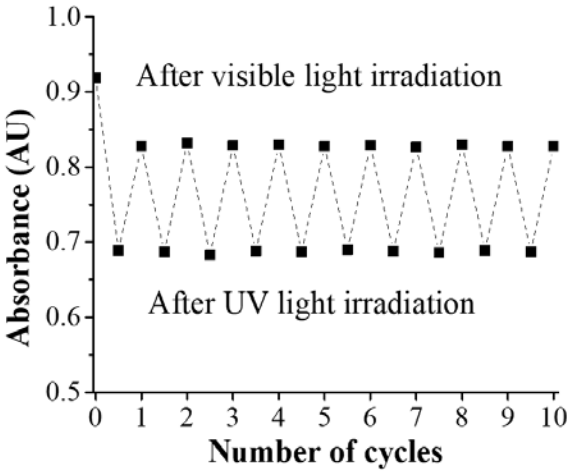

Fig. S4 UV and visible light-induced photoisomerization cycles of the PEA-2 film at 25 °C.

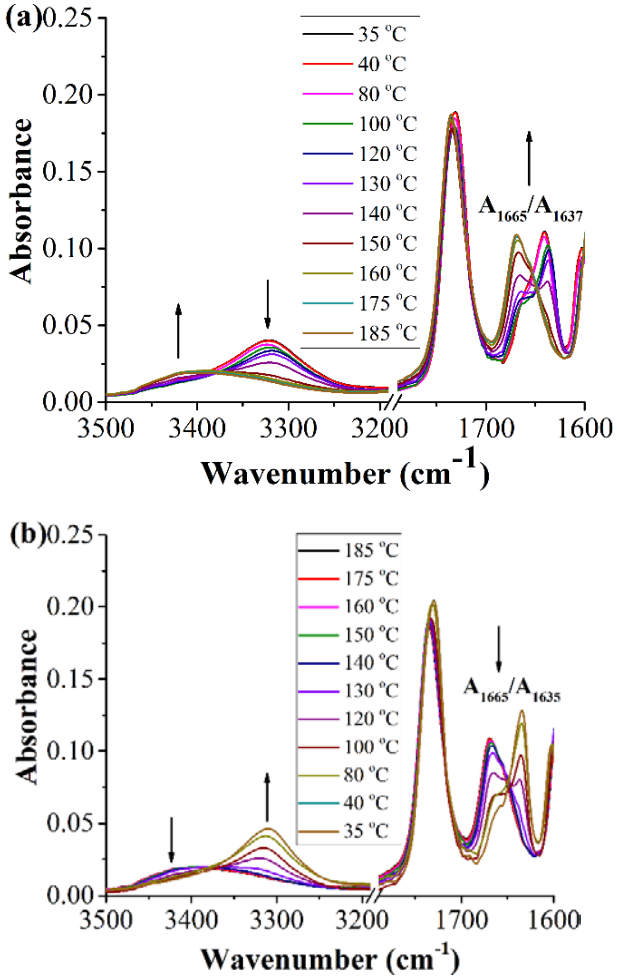

Fig. S5 FT-IR spectra of PEA-2b at different temperatures during the heating (a) and cooling (b) processes.

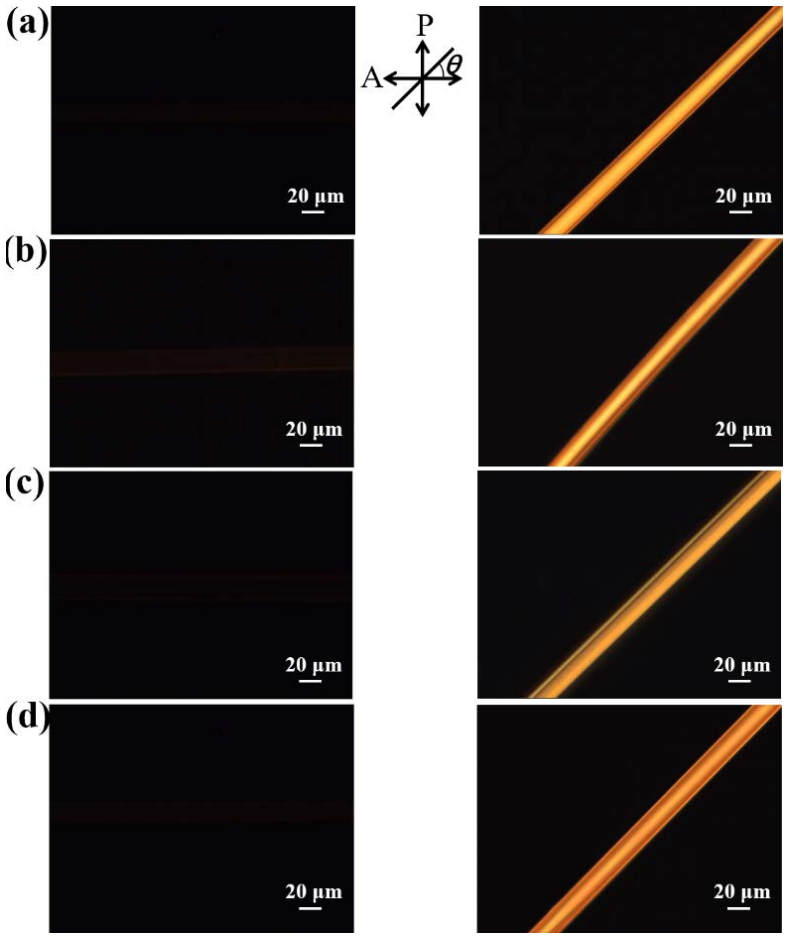

Fig. S6 POM images of the textures of PEA-4-*t* [*t* = 0.5 h (a), 1 h (b), 6 h (c), and 12 h (d)] fibers taken at room temperature. Sample angle to the analyzer: $\theta = 0^{o}$ (left); $\theta = 45^{o}$ (right).

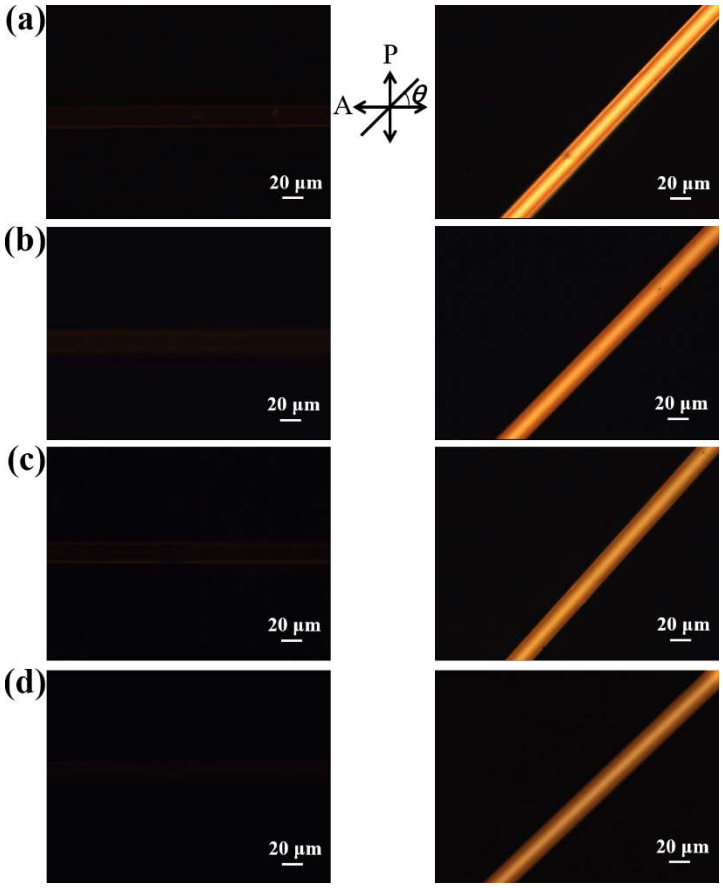

Fig. S7 POM images of the textures of the azo polymer [PEA-4 (a), PEA-6 (b), PEA-2b (c), and PEE-2 (d)] fibers taken at room temperature. Sample angle to the analyzer: $\theta = 0^{o}$ (left); $\theta = 45^{o}$ (right).

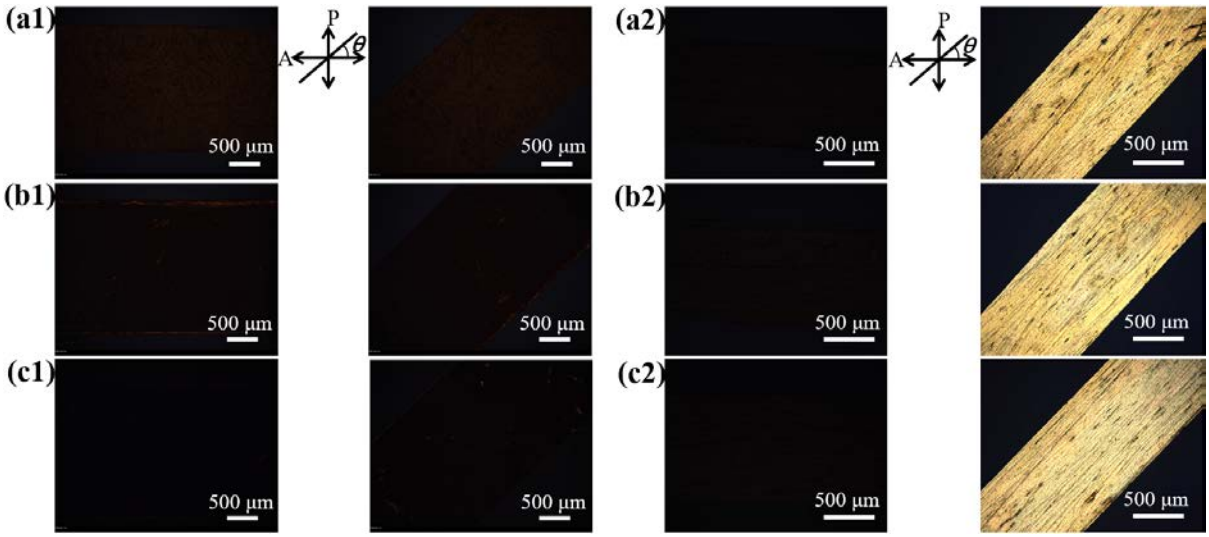

Fig. S8 POM images of the textures of the unstretched (a1,b1,c1) and stretched (a2,b2,c2) PEA-4 film (a1,a2), PEA-6 film (b1,b2), and PEE-2 film (c1,c2) taken at room temperature. Sample angle to the analyzer: $\theta = 0^{o}$ (left); $\theta = 45^{o}$ (right).

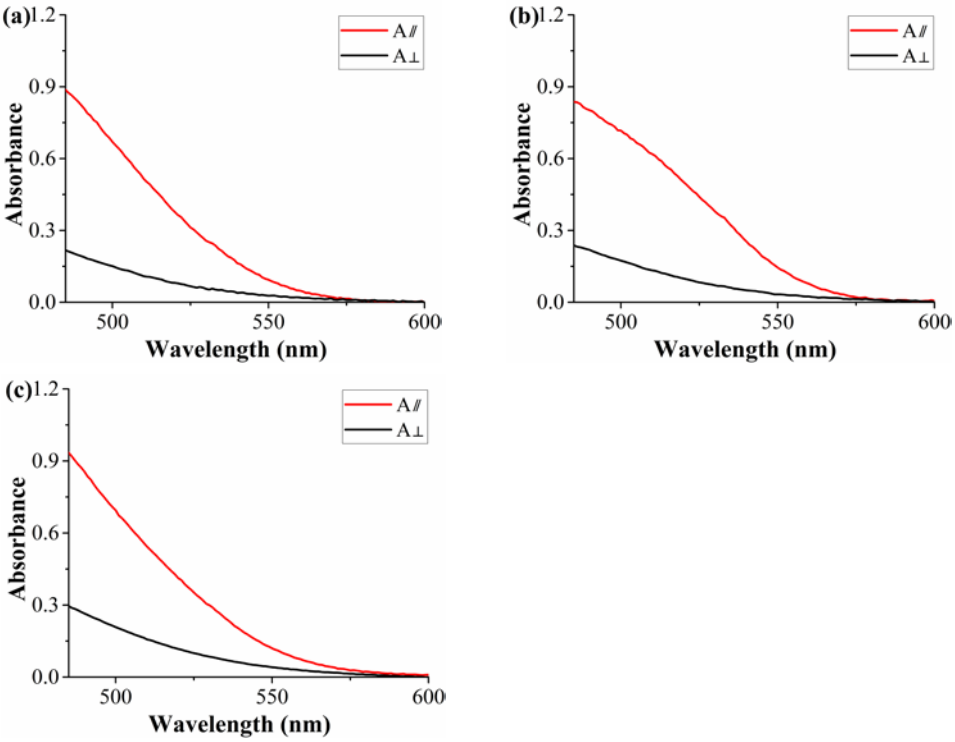

Fig. S9 Polarized absorption spectra of the uniaxially oriented PEA-2 film (a), PEA-4 film (b), and PEA-6 film (c). The strain and thickness of the films are 235% and about 10 μm, respectively.

Table S3 The order parameters of the uniaxially oriented PEA-*n* (*n* = 2, 4, 6) films derived from their polarized absorption spectra

entry	sample [a]	$A_{//}$ [b]	$A_{\perp}$ [b]	*S* [c]
1	uniaxially oriented PEA-2 film	0.65	0.14	0.55
2	uniaxially oriented PEA-4 film	0.75	0.18	0.51
3	uniaxially oriented PEA-6 film	0.70	0.21	0.44

[a] The strain and thickness of the films are 235% and about 10 μm, respectively. [b] $A_{//}$ and $A_{\perp}$ refer to the absorbance (at 500 nm) obtained with incident light polarized parallel and perpendicular to the stretching direction of the films, respectively. [c] *S* refers to the order parameters of the uniaxially oriented PEA films.

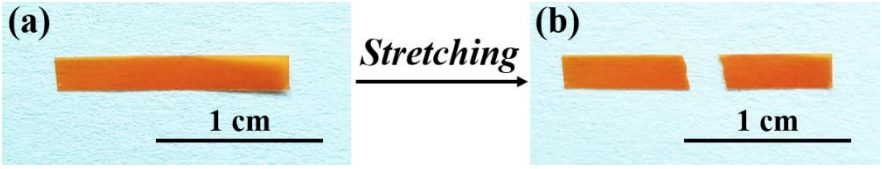

Fig. S10 The photo images of an unstretched PEA-2b film (a) and the resulting broken PEA-2b film upon stretching (b).

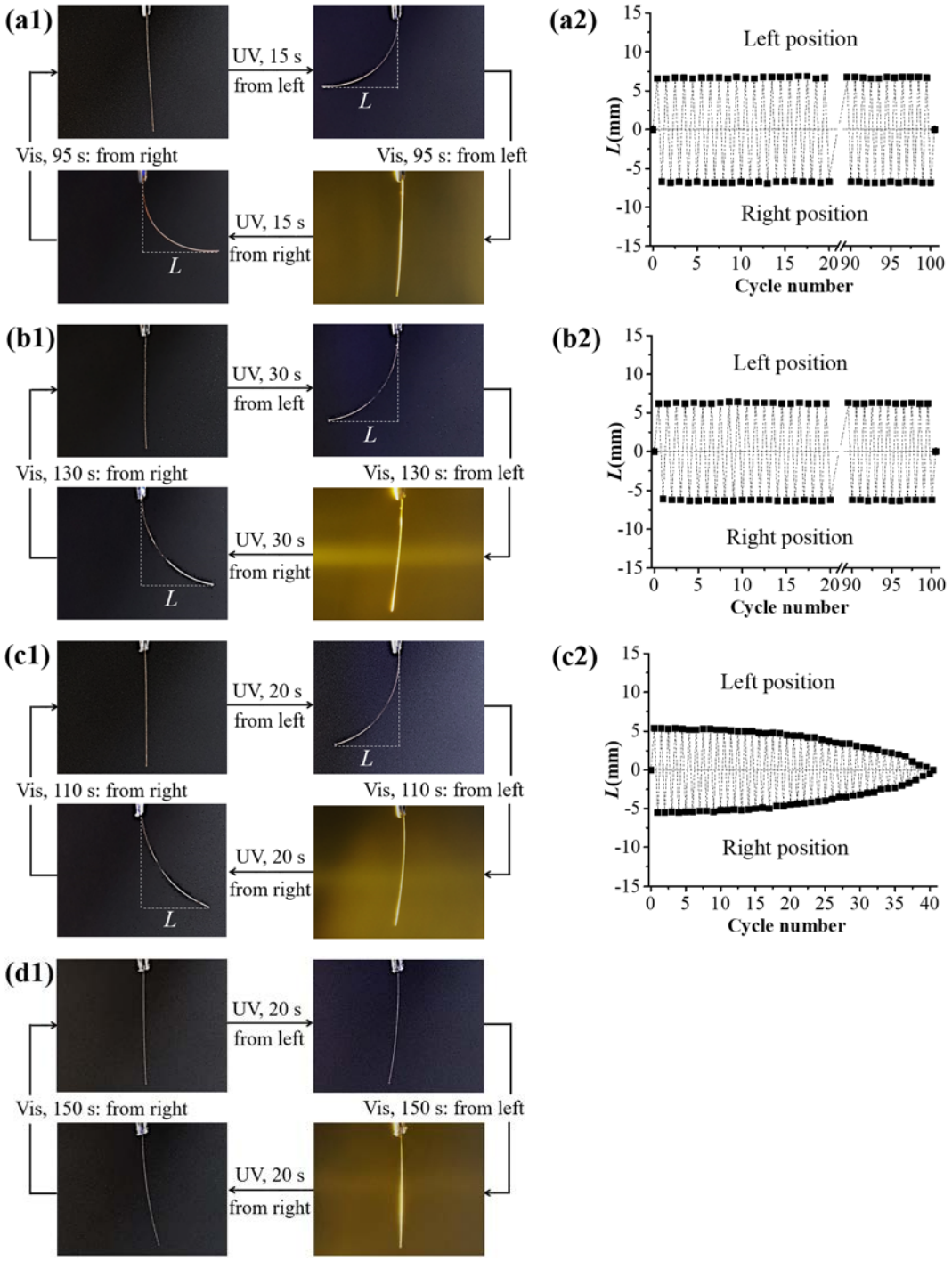

Fig. S11 (a1-d1) Photographs of the azo polymer [PEA-4 (a1), PEA-6 (b1), PEA-2b (c1, the first photomobile cycle), and PEE-2 (d1)] fibers that exhibit photoinduced bending and unbending upon irradiation with 365 nm UV light (40 mW cm^{-2}) and visible light (λ > 510 nm, 30 mW cm^{-2}) at 25 °C. (a2-c2) Reversible deformation of the azo polymer [PEA-4 (a2), PEA-6 (b2) and PEA-2b (c2)] fibers characterized by tracing the bent distances from their straight states at 25 °C. The sizes (length × diameter) of azo polymer fibers: PEA-4 fiber (10 mm × 21 μm), PEA-6 fiber (10 mm × 21 μm), PEA-2b fiber (10 mm × 21 μm), and PEE-2 fiber (10 mm × 20 μm).

Table S4 Photoinduced bending and unbending data of the unaxially oriented PEA-4-*t* fibers

polym. time *t* (h)	UV-induced bending rate (s) [a]	Vis-induced unbending rate (s) [b]	bending amplitude (mm)	cycle number
0.5	20 ± 2	130 ± 9	6.8 ± 0.4	＞100
1	18 ± 2	115 ± 8	7.0 ± 0.4	＞100
3	**15 ± 2**	**95 ± 7**	**6.8 ± 0.4**	**＞100**
6	20 ± 2	105 ± 7	6.5 ± 0.4	＞100
12	30 ± 2	130 ± 8	6.3 ± 0.5	＞100

[a] The time for the fibers to reach their maximum bending. [b] The time for the bent fibers to restore their initial straight states.

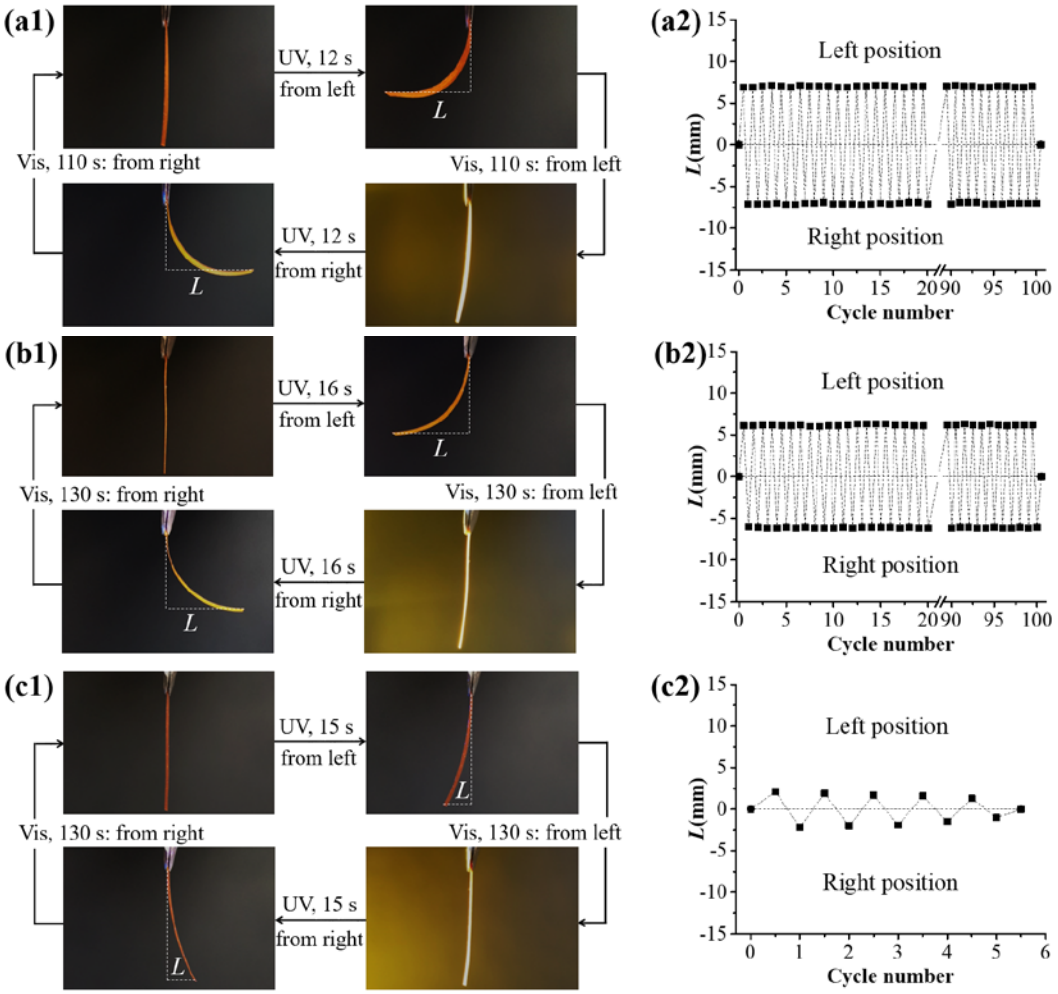

Fig. S12 (a1-c1) Photographs of the stretched azo polymer [PEA-4 (a1), PEA-6 (b1), and PEE-2 (c1, the first photomobile cycle)] films that exhibit photoinduced bending and unbending upon irradiation with 365 nm UV light (40 mW cm^{-2}) and visible light (λ > 510 nm, 30 mW cm^{-2}) at 25 °C. (a2-c2) The reversible deformation of the stretched azo polymer [PEA-4 (a2), PEA-6 (b2), and PEE-2 (c2)] films characterized by tracing the bent distances from their straight states at 25 °C. The sizes (length × width × thickness) of the stretched films are as follows: PEA-4 film (10 mm × 1 mm × 38 μm), PEA-6 film (10 mm × 1 mm × 35 μm), and PEE-2 film (10 mm × 1 mm × 36 μm).

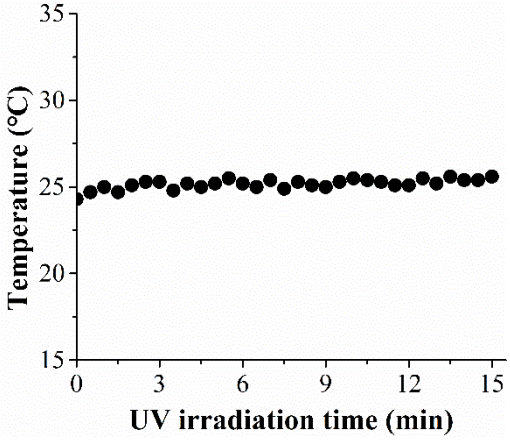

Fig. S13 Time dependence of the temperature of the stretched PEA-2 film under the continuous UV light irradiation (40 mW cm^{-2}) [the film temperature was determined by using a Fluke TiS10 Infrared Camera 9Hz (Fluke International Corporation)].

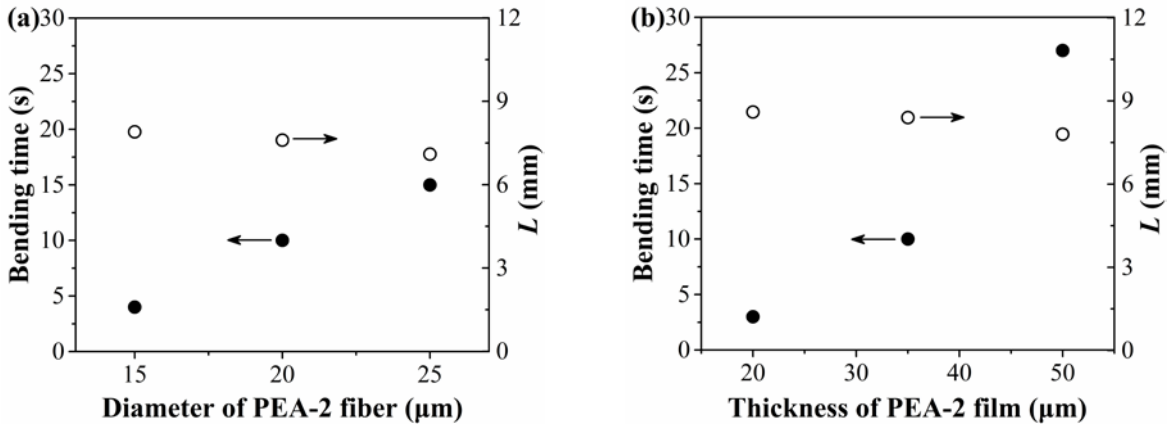

Fig. S14 Effect of the diameters of the uniaxially oriented PEA-2 fibers (a) and the thickness of the uniaxially oriented PEA-2 films (b) on their bending times (i.e., the times required to reach the maximum bending) and amplitudes upon their exposure to 365 nm UV light (40 mW cm^{-2}) at 25 ºC. The length of the fibers is 10 mm, and the length and width of the films are 10 mm and 1 mm, respectively.

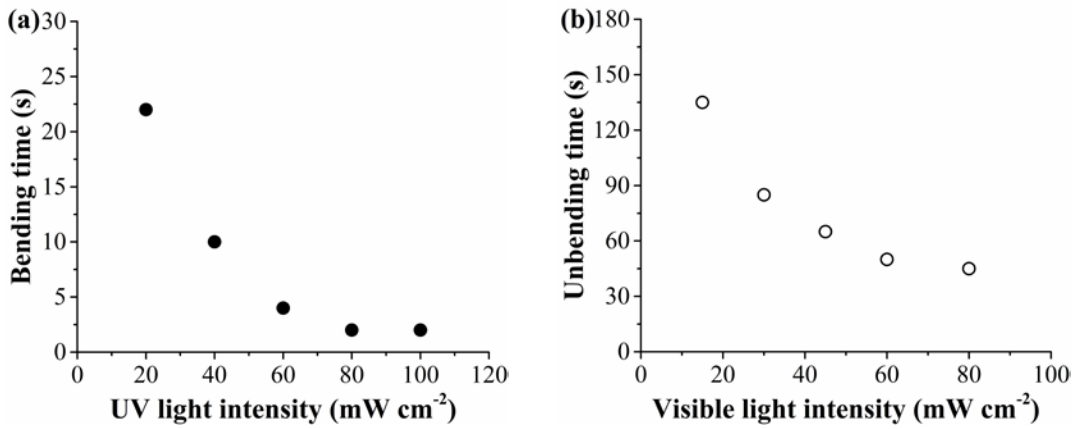

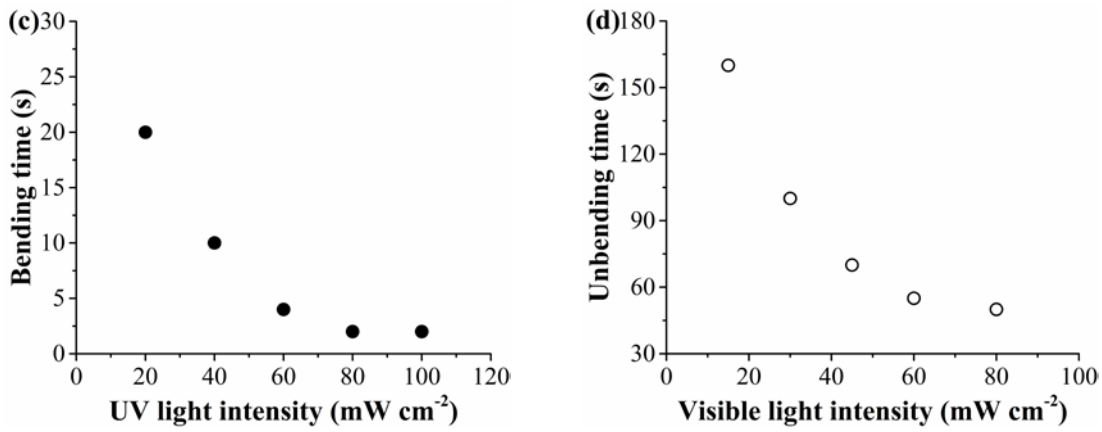

Fig. S15 Dependence of the photomobile rates of the uniaxially oriented PEA-2 fiber (10 mm × 21 μm) (a,b) and film (10 mm × 1 mm× 36 μm) (c,d) on the UV (a,c) and visible (b,d) light intensity.

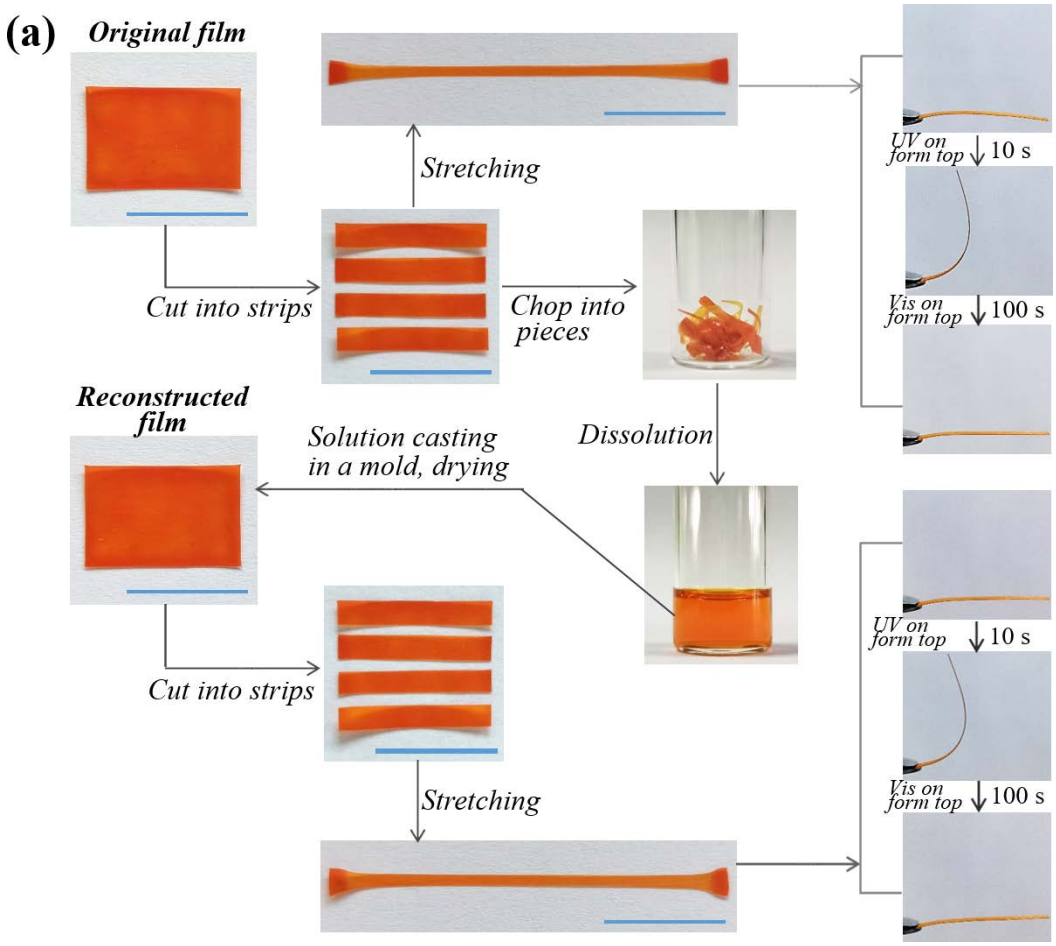

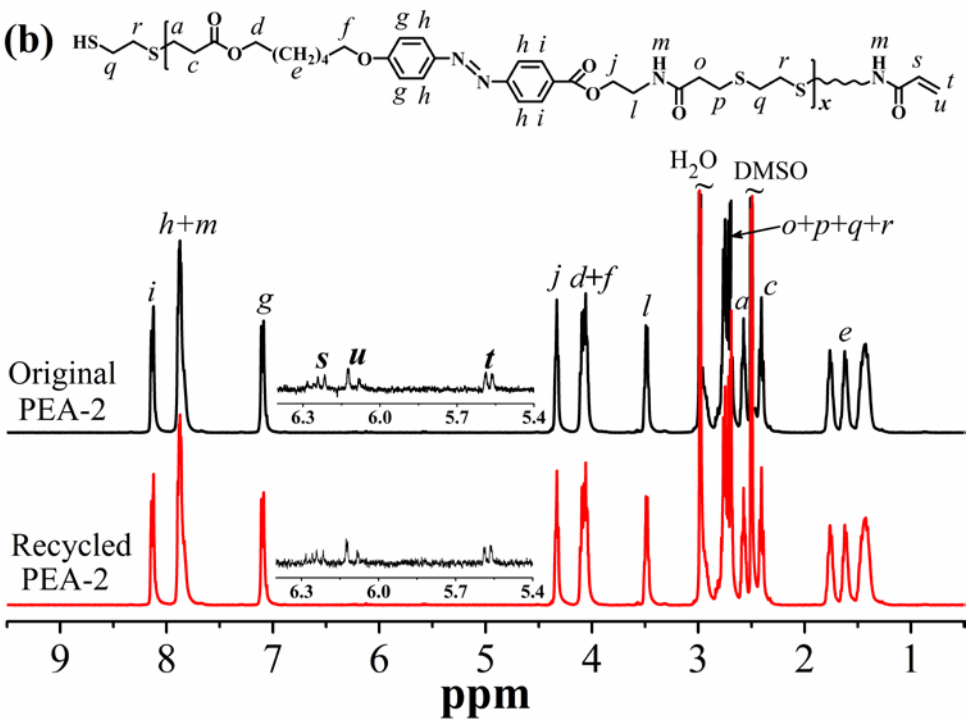

Fig. S16 (a) Reprocessability of the photomobile PEA-2 film. Reconstructing a PEA-2 film by first dissolving the chopped PEA-2 film into hexafluoroisopropanol, adding the solution into a Teflon mold, evaporating the solvent, cutting the peeled film into strips, and then stretching one to 235% strain (all processes at room temperature). The reconstructed stretched PEA-2 strip (10 mm × 1 mm × 37 μm) shows reversible bending/unbending (over 100 cycles) similar as the original PEA-2 strip (10 mm × 1 mm × 35 μm) upon exposure to UV (365 nm, 40 mW cm^{-2}) and visible light (λ > 510 nm, 30 mW cm^{-2}). Scale bars are 1 cm. (b) ^{1}H NMR spectra of the original PEA-2 and the recycled PEA-2 in DMSO-d_6 determined at 80 °C.

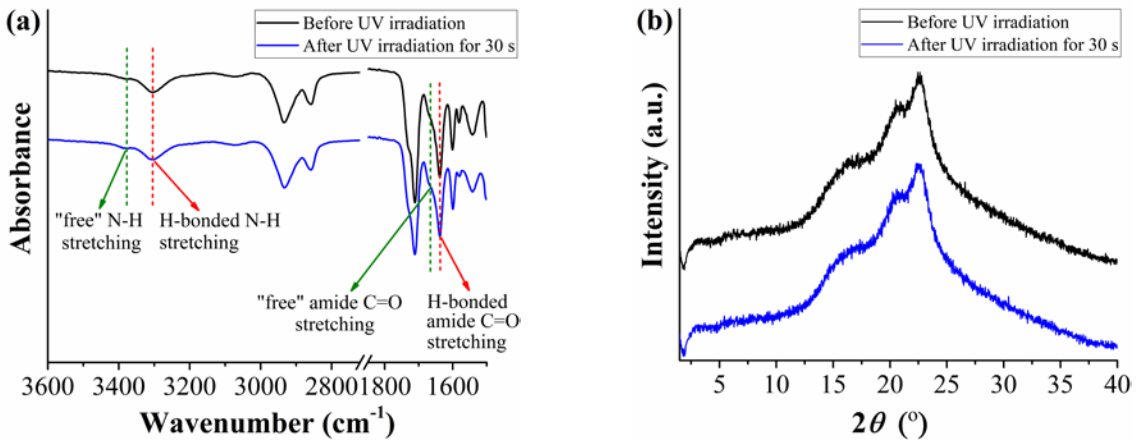

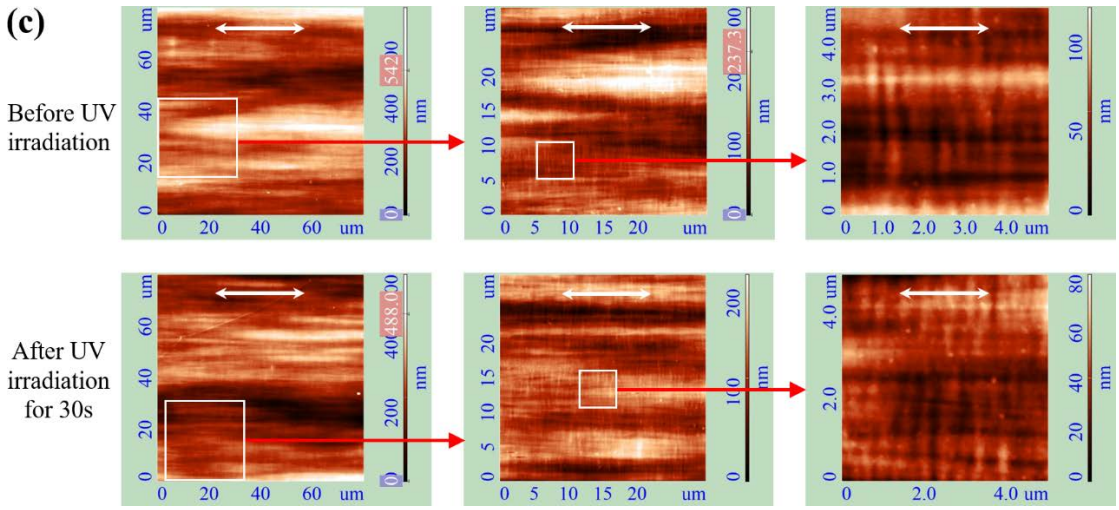

Fig. S17 FT-IR (a) and XRD (b) spectra as well as AFM images (c) of the uniaxially oriented PEA-2 films at the same side measured before UV light irradiation and immediately after UV light (40 mW cm^{-2}) irradiation for 30 s at 25 °C, respectively. The sizes of PEA-2 films are 10 mm × 1 mm × 36 μm.

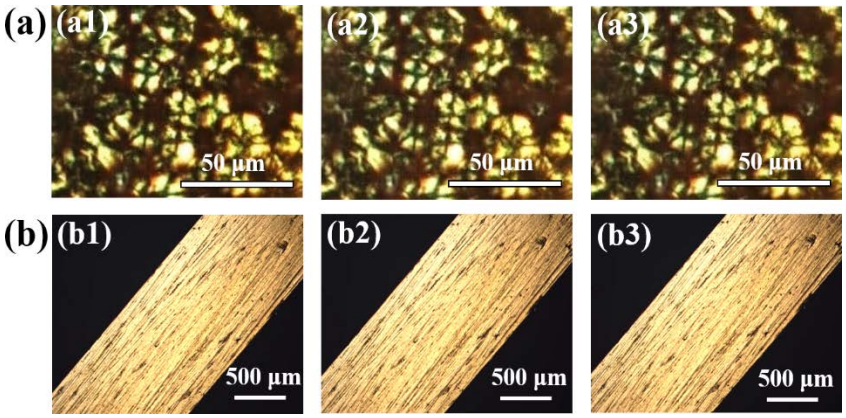

Fig. S18 POM images of the unstretched (a) and stretched (b) PEA-2 films before UV light irradiation (a1,b1), immediately after 365 nm UV light irradiation (40 mW cm^{-2}) for 30 s (a2,b2), and after irradiating the films (they were irradiated with UV light for 30 s) with visible light (λ > 510 nm, 30 mW cm^{-2}) for 120 s (a3,b3).